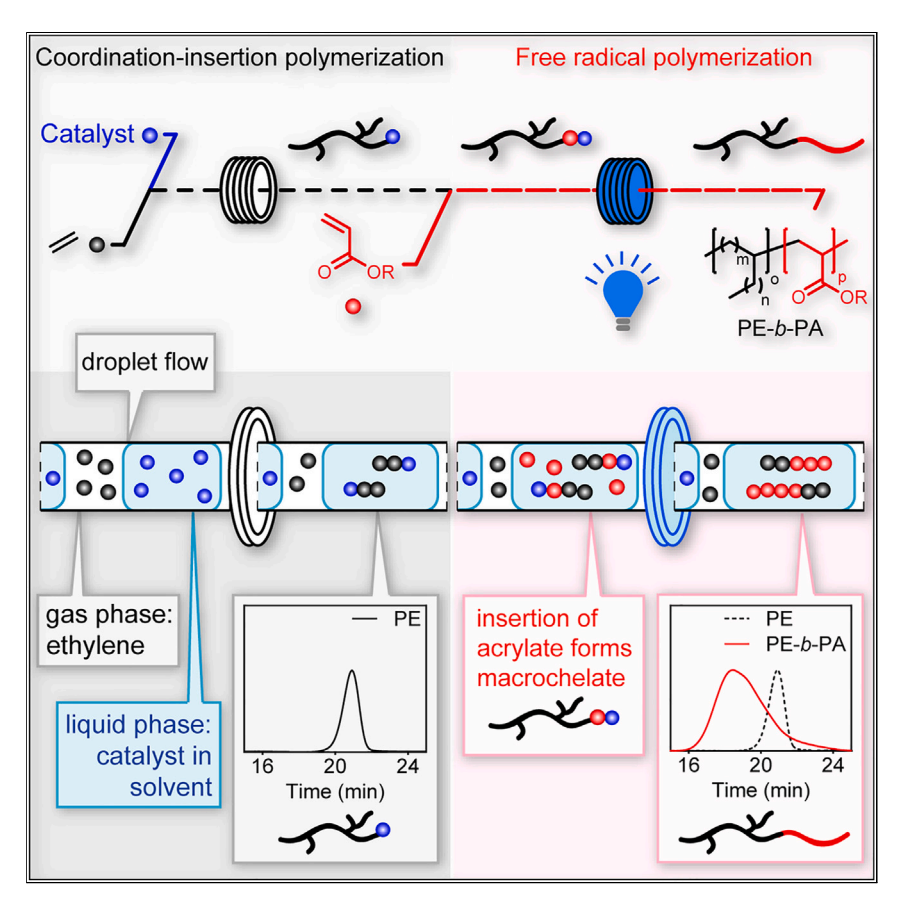




Article

Synthesis of polyethylene-polyacrylate block copolymers in continuous flow



A range of polar polyolefin block copolymers is prepared in continuous flow using a combination of coordination-insertion and radical polymerization, utilizing a droplet flow system in which the gaseous phase participates in the synthesis.

Stephen Don Sarkar, Huong Dau, Eva Harth

harth@uh.edu

Highlights

Combination of coordinationinsertion and radical polymerization in continuous flow

Block copolymer synthesis utilizing a droplet flow of gaseous monomer

A single catalyst facilitates the synthesis of polar polyolefin block copolymers

Sarkar et al., Chem 10, 2872–2886 September 12, 2024 © 2024 Elsevier Inc. All rights are reserved, including those for text and data mining, Al training, and similar technologies.

https://doi.org/10.1016/j.chempr.2024.05.016









Article

Synthesis of polyethylene-polyacrylate block copolymers in continuous flow

Stephen Don Sarkar, 1 Huong Dau, 1 and Eva Harth 1,2,*

SUMMARY

Continuous flow reactions for the synthesis of block copolymers are a useful synthetic strategy because they provide better control over the polymerization reactions with easy scaling-up ability. Herein, a continuous flow system has been designed to combine two adverse polymerization processes, coordination-insertion using gaseous ethylene and free radical polymerization utilizing monomers of the acrylate family, to form polar polyethylene block copolymers. We demonstrate that a gas-liquid heterogeneous droplet flow system can lead to a successful living ethylene polymerization in which the gaseous component contains the reactive monomer. The addition of acrylates switches the reaction location to the liquid phase through the formation of a macroinitiator for the radical pathway and retarding the ethylene polymerization. We demonstrate that block copolymer segments can engage all phases of the droplet flow system and enable the synthesis of polar polyolefin block copolymers employing a single catalyst.

INTRODUCTION

Continuous flow synthesis offers several advantages over traditional batch syntheses, such as high precision, excellent reproducibility, constant temperature conditions, and enhanced safety when handling hazardous chemicals. ^{1–7} In addition, the uninterrupted operation of continuous flow reactors enables large-scale production, ranging from milligrams to kilograms of materials utilizing the same equipment. Conversely, upscaling in conventional batch processes often requires the installation of new equipment, and in some cases, it can be detrimental to overall product quality. ^{4,6,8}

The utilization of flow chemistry has revolutionized drug development and translated organic small-molecule synthesis to the industrial scale. $^{9-11}$ However, synthesizing macromolecules in continuous flow imposes a higher level of complexity because the fluid dynamics in the tubular reactor influence the structure and composition of polymer segments. $^{12-14}$ Due to the higher viscosity of typical polymer solutions, the velocity profile of polymerization reactions forms a greater parabolic laminar flow with broader residence times distribution (RTD) compared with analogous small-molecule reactions and affects the conversion of monomers, molecular weight (M_n), and dispersity (D) of polymers. $^{15-18}$ Therefore, often a higher D is observed compared with batch polymerization. $^{12,19-23}$ To retain the narrow D of chain polymerizations, all chains need to experience the same conditions, which is challenging to achieve in the laminar flow. 12,15,24 To remedy these shortcomings, a plug-flow system in which a droplet flow is maintained will allow for more uniform reaction conditions, resulting in a narrow RTD. 25,26 Here, a gaseous phase confines the liquid reaction droplets and affords a circulating homogeneous reaction pattern

THE BIGGER PICTURE

Polar polyolefin block copolymers containing segments of polyolefins and polyacrylates are highly desired in energy storage and plastic recycling applications. Controlling each segment to form a variety of compositions and providing practical syntheses are crucial to advancing these materials for the desired applications. Specifically, continuous flow reactions have been investigated to transform bulk reactions to a larger scale with consistent and reproducible outcomes.

Here, we present the first example of how a polar polyolefin block copolymer synthesis can be realized in the continuous flow, affording block copolymers in a range of different molecular weights and acrylate block content.







to yield well-controlled polymerization. ^{12,15,25,27,28} For instance, during a photo-induced electron/energy transfer reversible addition-fragmentation transfer (PET-RAFT) polymerization in droplet flow, Boyer et al. observed a significant increase in the consistency of monomer conversion, composition, and *D* in the produced polymers over time compared with traditional continuous flow. ¹⁵ Leibfarth and coworkers demonstrated that using the droplet flow for chain reactions in the case of RAFT and ring-opening polymerization (ROP) showed *D* values that matched with polymerizations conducted in the small-scale batches. ¹² The advantages of a droplet flow have also been investigated with immiscible solvent combinations to isolate the reaction droplet for homo- and copolymerization of polyacrylates (PAs). ^{24,29,30}

However, block copolymer (BCP) synthesis is regularly conducted in laminar flow systems, using the same polymerization mechanism, for example, controlled radical polymerization (CRP), 31-40 ionic polymerization, 41-45 and ROP46-48 throughout adding one monomer after another in a linear setup of reactors. The increasing viscosity, resulting in an increasing θ is mostly maintained by keeping the M_n of the di- and multi-blocks in low M_n regions, ranging, for example, from 1-10 kDa. 32,33,43,47,49,50 In addition, a combination of polymerization methods in which one block is prepared through a polymerization technique different from the second block is limited (Figure 1A). Junkers and co-workers showed such BCP preparation by combining different methods of CRP, in which one polymer segment is prepared by either atom transfer radical polymerization (ATRP) or RAFT polymerization with subsequent end-functionalization, and the prepared blocks were then combined by click chemistry to form di-BCPs. 51 In another example, Zhu et al. synthesized poly(ε-caprolactone)-b-poly(N-vinylpyrrolidone) through sequential ROP and free radical polymerization (FRP).⁵² However, there is no example known in which coordination-insertion and FRP have been combined in the continuous flow to form polar polyolefin BCPs (Figure 1B).

One of the challenges to combine such pathways is the adverse properties of the involved monomer families, gaseous olefins, and liquid acrylates. There has been no investigation using the gaseous mobile phase as a monomer carrier and facilitating at the same time a droplet flow in which the monomers of the gaseous phase participate in chemical transformation themselves (Figure 1C). Gaseous monomers have not been translated to the continuous flow, and only tubular reactors ^{53–55} and fluidized-bed reactors ^{56,57} on an industrial scale for high-temperature free radical reactions are known for olefin polymerizations. Recently, Chen and coworkers synthesized alternative copolymers and BCPs of chlorotrifluoroethylene (CTFE) and vinyl ester/amide in a flow system through PET-RAFT, where a saturated CTFE solution was prepared by bubbling gaseous CTFE into diethyl carbonate to perform the polymerization reaction. ⁵⁸

Herein, we present the development of a heterogeneous droplet flow system that carries monomers in both the gaseous and liquid phases separately to promote the formation of BCPs containing polyethylene (PE) and PA segments (Figures 1B and 1D). This can be made possible through the development of a method that allows for a switching of the insertion pathway forming the polyolefin and initiating the radical pathway in a single catalytic system, known as metal-organic insertion light-initiated radical (MILRad) polymerization. ^{59–62} Here, a cationic diimine Pd^{II} complex facilitates the living coordination-insertion polymerization (CIP) to synthesize a PE block. Subsequently, a Pd-PE-macrochelate is formed after the insertion of an acrylate monomer, which generates a macroradical species through the homolytic

¹Center of Excellence in Polymer Chemistry (CEPC), Department of Chemistry, University of Houston, Houston, TX 77204, USA

https://doi.org/10.1016/j.chempr.2024.05.016

²Lead contact

^{*}Correspondence: harth@uh.edu





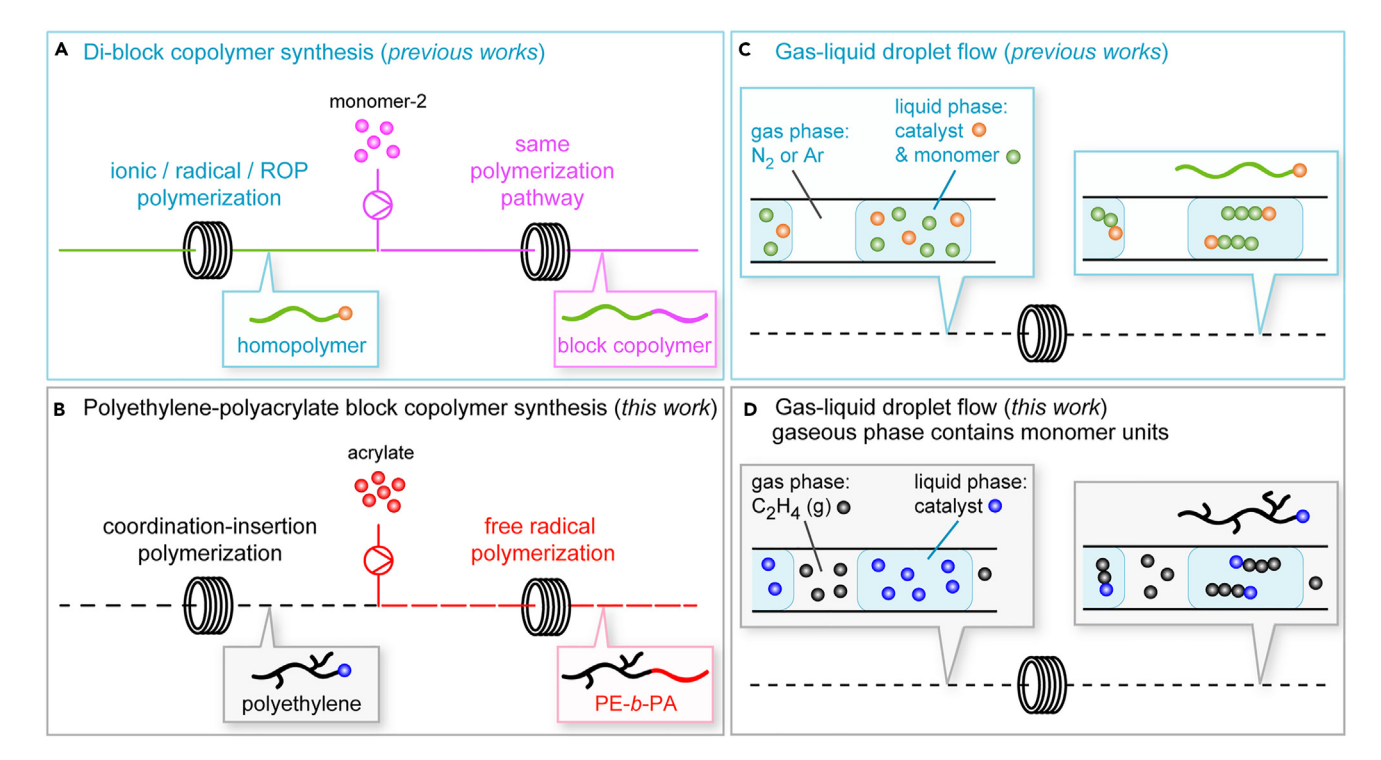


Figure 1. Polymerization in continuous flow

(A and B) Comparison in di-block copolymer synthesis using the same or different polymerization pathways for both blocks. (C and D) Comparison in utilization of gas phase in gas-liquid droplet flow systems.

cleavage of Pd-C upon blue light irradiation (\sim 457 nm) to initiate FRP in the presence of excess acrylate monomers, forming the second block of PE-b-PA di-BCPs. A single catalyst mediates CIP and FRP sequentially, bypassing the multistep syntheses involving post-functionalization processes.

In this work, we first investigate PE homopolymerization through CIP utilizing a Brookhart type α -diimine Pd^{II} complex (C1) in a continuous flow reactor (Figure 2), and a detailed kinetic investigation varying the system's parameters is performed to establish the living window of the olefin polymerization. Using a droplet flow system, in which the gaseous phase contains ethylene, the effect of residence time, gas flow rate, gas pressure, and catalyst concentration on PE polymerization is investigated. It is shown that each parameter can adjust the M_n and yield and enables polymerization at the gas-liquid droplet interface.

Second, we separately study the LRad polymerization of methyl acrylate (MA) and its kinetic behavior employing the same catalyst in the liquid phase of a continuous flow system. Here, in laminar flow, the influence of residence time and concentrations of monomer and catalyst on the M_n and yield of poly(MA) (PMA) is investigated. Next, a sequential combination of these flow systems is adopted to merge these two reaction pathways and form the PE-PMA BCP (PE-b-PMA). A study to optimize the Pd-PE-macrochelate opening and faster radical initiation is evaluated through the presence of additional quantities of the ancillary ligand. A radical trapping experiment is carried out in the presence of MA and tetramethylpiperidine-N-oxyl (TEMPO) to validate the formation of the PE radical macroinitiators. Several PE-b-PAs are synthesized to establish a new route for preparing advanced polymeric materials, such as polar polyolefin BCPs.



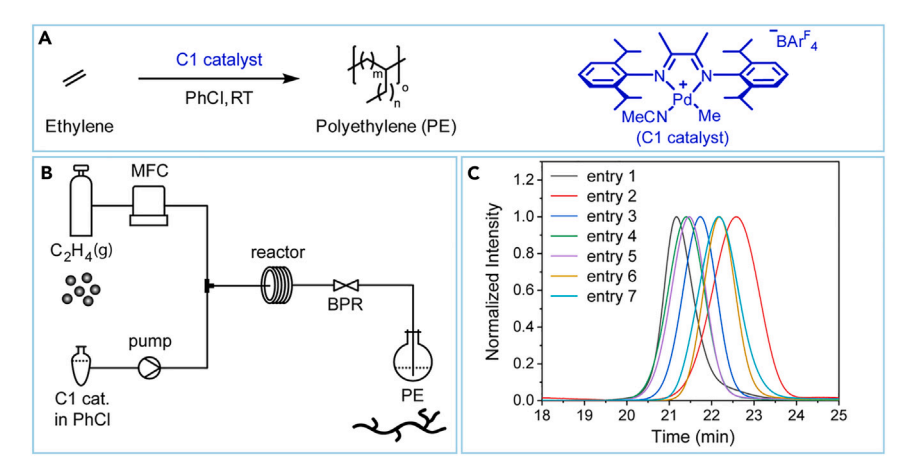


Figure 2. Synthesis of polyethylene homopolymer in the continuous flow reactor

- (A) Coordination-insertion polymerization of ethylene utilizing C1 catalyst.
- (B) Schematic diagram of the continuous flow reactor for ethylene polymerization.
- (C) GPC traces of PE homopolymers of Table 1.

RESULTS AND DISCUSSION

Synthesis of PE homopolymer in continuous flow

In the CIP of ethylene, a gas-liquid heterogeneous system was utilized in the form of a droplet flow consisting of catalyst solvent droplets separated by the ethylene monomer gas phase (Figures 1D, 2, and S1). This study investigated the effects of various flow parameters, such as residence time, monomer concentration, and catalyst concentration, in detail for optimization of PE homopolymer synthesis, summarized in Table 1. It was found that the residence time of the reaction has a significant impact on the average M_n and the yield of PE homopolymers. Residence time in flow chemistry refers to the time a reagent or reactant spends inside a flow reactor during a chemical reaction. The residence time can be regulated by adjusting the flow rate of feed solutions or the length of the reactor. In the initial setup, testing suitable residence times in the flow, we tried to match the same reaction times of CIP in the flow with the batch using similar experimental conditions to compare the M_n in the two modes of reaction procedures. We found that the M_n of the batch reactions are similar to the reactions that were run in the flow at the same residence times when we targeted M_n ranging from 5–40 kg/mol. We varied the pump flow rate and length of the tubing to further modulate the residence

Table 1. Insertion polymerization of ethylene in the presence of C1 catalyst in the continuous flow reactor											
Entry ^a	Length of reactor (m)	Pump flow rate (mL/min)	Res. time (min)	Conc. of C1 Cat. In PhCl (µmol/mL)	Gas flow rate (mL/min) ^b	BPR (Psi)			Yield (mg)	TOF (×1000/h)	No. of branches (per 1,000 C) ^d
1	1.5	0.15	7	2.10	6	250	14.28	1.06	75	2.43	103
2	1.5	0.30	4	2.10	6	250	5.68	1.07	87	2.47	106
3	3.0	0.30	6	2.10	6	250	11.63	1.04	128	2.42	107
4	3.0	0.30	6	1.40	6	250	13.74	1.05	113	3.20	109
5	3.0	0.30	6	1.40	6	100	13.45	1.05	109	3.09	106
6	3.0	0.30	7	1.40	3	100	9.03	1.04	70	1.70	107
7 ^e	3.0	0.30	7	1.40	3	100	9.03	1.06	143	1.74	104

^a30 min reaction time.

^bEthylene gas flow was controlled by a mass flow controller.

 $^{^{\}circ}$ Molecular weight (M_n) and dispersity (D) were determined by gel permeation chromatography (GPC) analysis with samples ran in tetrahydrofurane (THF) at 40° C calibrated to polystyrene standards.

^dDetermined by ¹H-NMR in CDCl₃ at 25°C.

e60 min reaction time.





time and with this the M_n of the PE. Now, increasing the flow rate of the C1 catalyst solution from 0.15 to 0.30 mL/min reduced the residence time to \sim 50% (entries 1 and 2), which led to a decrease in M_n (14.28 to 5.68 kg/mol) of the product almost in the same ratio. Conversely, these outcomes were enhanced (roughly double) with an increase in residence time from \sim 4 to \sim 6 min resulting from increasing the reactor length from 1.5 to 3.0 m (entries 2 and 3). Because the greater residence time offers an extended duration of reaction, it ensures a longer span for chain propagation to obtain higher M_n and yield.

Interestingly, CIP of ethylene with higher catalyst concentration resulted in PE chains of lower M_n (entries 3 and 4). An excess of catalyst led to a faster initiation and propagation of monomer units, which increased the polymer yield. Nevertheless, this extended initiation consequently created an event of multiple competing polymerizations, where the individual polymer chains received fewer monomer units and had less time to grow before they were quenched. This shorter chain growth resulted in shorter polymer chains with lower average M_n . On the contrary, an increase of the ethylene gas injection rate (3 to 6 mL/min) with similar residence time ensures an additional amount of monomer units in the reaction, corresponding to extended propagation and chain growth leading to enhancement of M_n and yield of PE, and was observed in the cases of entries 5 and 6.

The C1 complex was exploited to perform the CIP of ethylene in four major steps: initiation, chain propagation, metal migration through the polymer chain (chain walking), and chain transfer (Figure S2). The insertion pathway initiates through the coordination of the C1 complex with ethylene monomer, and further successive coordination and insertion of ethylene forms the PE chain. The chain-walking characteristic of the Pd^{II} complex results in an agostic intermediate II, which can proceed to further coordination-insertion with monomers to yield the stable π -complex III or can undergo β -hydride elimination to form IV. These Pd^{II} ethylene π -complexes (III and VI) are the resting state of this pathway, indicating that the insertion step is the rate-limiting step. Therefore, the rate of polymerization and the degree of branching are independent of system pressure. 63-65 As a result, changing the backpressure regulator in the flow system did not largely impact the production of PE homopolymer except for a subtle increase in M_n and yield (entries 4 and 5). Finally, continuing the reaction for a longer time from 30 to 60 min without altering any other parameters (entries 6 and 7) yielded homopolymers of similar molecular weight $(M_n \approx 9.03 \text{ kg/mol}; \mathcal{D} \approx 1.04)$ but produced a higher yield (around 2-fold) as twice the amount of feed solution was consumed and underlines the easy scalability of PE in this method.

A further kinetic study of PE chain extension based on the residence time varying the flow rate of the reactants was performed to investigate the living window of PE homopolymerization (Table S1). In Figure 3B, a linear agreement, following first-order kinetics, between the increase in average M_n (5.88 to 42.19 kg/mol) and the increase of resident time (3 to 21 min), was observed while maintaining a narrow \mathcal{D} ($\mathcal{D} = M_w/M_n \approx 1.05$). This relation evidenced the subsequent monomer propagation for continuing the PE chain growth within a living time frame over the β -hydride elimination and chain transfer. ^{61,66,67} In the case of living polymerization, after a fast chain initiation, a constant rate of chain propagation is maintained in the absence of chain termination. As a result, a linear relationship between the M_n of the polymers and reaction time with narrow \mathcal{D} is observed. Therefore, we can conclude that PE polymerization in the flow reactor is a living process, and we can aim for any desired length of a PE segment by varying the residence time.



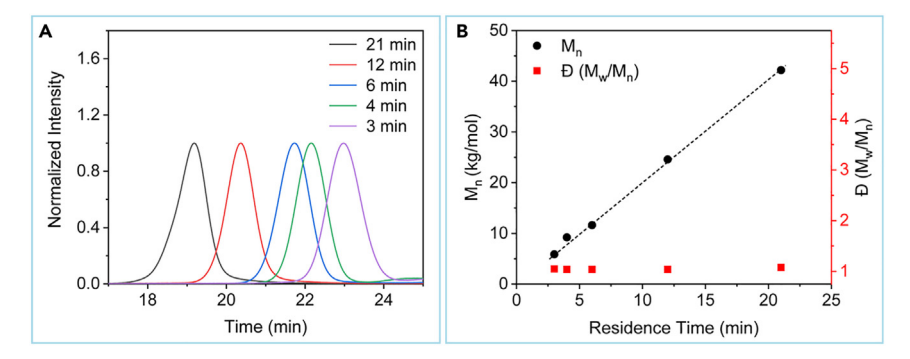


Figure 3. Kinetic study of PE homopolymerization based on residence time varied with the flow rate of catalyst solution (A) GPC traces of PE homopolymers for different residence times (Table S1).

(B) M_n vs. residence time plot evidenced living polymerization of ethylene.

Although the experimental setups of the continuous flow reactor and batch process are entirely different, we examined if the experimental conditions impact the characteristics of the homopolymer when choosing the same catalyst concentration and reaction time. The resulting PE homopolymers, conducted in the batch and the flow, are summarized in Figure S5 and Table S2. In both processes, the obtained products were similar in characteristics, such as M_n , D, and TOF. Therefore, we can conclude that the experimental conditions do not alter the polymerization results. However, in the case of batch reactions, every reaction is tailored toward its specific reaction volume and the defined range of its reaction vessel. Therefore, we can argue that the flow system is well capable in formulating the desired product as a batch reaction while offering easier scalability and better control in preparation.

Synthesis of PMA homopolymer in continuous flow

PMA homopolymers were prepared through a LRad pathway employing the same Pd^{II} diamine C1 catalyst. The previously reported mechanistic study (Figure S6) illustrated that the initiation of the reaction involves a 2,1 insertion of MA (excess) displacing the ancillary ligand acetonitrile (MeCN) from the catalyst to yield a four-membered intermediate, which is subsequently rearranged to form a stable six-membered chelate via chain walking. The presence of Lewis base (MeCN) aids the reopening of the chelate and Pd chain walk to the α -carbon, which is subsequently subjected to blue light (\sim 457 nm) irradiation to undergo the Pd-C bond homolysis to generate the radical species for further FRP of MA.^{68–70}

Similar to the CIP of ethylene, a similar investigation was conducted for the LRad reactions of MA by varying the parameters of the flow system to achieve the modulation in M_n . The initial residence time parameters were chosen based on the reaction times of LRad in the batch. Here (Figure 4; Table 2), increasing the residence time by changing the flow rate of the monomer and the catalyst solutions (entries 1 and 2) or the length of the reactor (entries 2 and 3) offered an extended period for chain propagation and enhanced the M_n and yield of the obtained PMA. On the other hand, increasing the catalyst concentration from 1.4 to 2.1 μ mol/mL resulted in a decrease in the M_n (118.86 to 72.02 kg/mol) of the prepared polymer. We suggest that the higher catalyst concentration generated a greater number of initiator radical species, initiating a greater number of polymer chains simultaneously (entries 3 and 4), and also increased termination rates as part of steady-state free radical kinetic behavior. However, increasing the monomer concentration promotes a higher monomer propagation to form a longer chain with higher M_n (entries 3 and 5). In the end, a comparison between entries 5 and 6 elucidates that only the extended





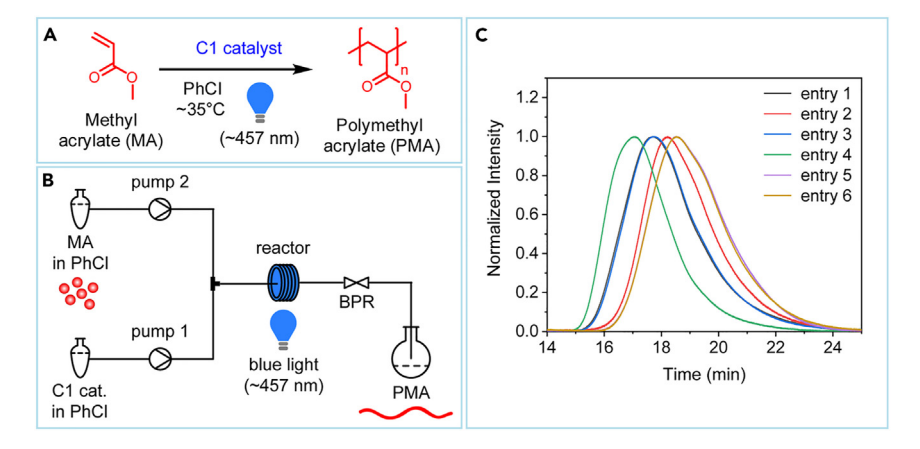


Figure 4. Synthesis of poly(methyl acrylate) homopolymer in the continuous flow reactor

(A) Light-initiated free radical polymerization of methyl acrylate employing C1 catalyst.

- (B) Schematic diagram of the continuous flow reactor for methyl acrylate polymerization.
- (C) GPC traces of PMA homopolymers of Table 2.

reaction time (30 to 60 min) utilizing a higher amount of feed solution without varying any other flow parameters can generate a higher amount of PMA homopolymers (0.49 to 1.03 g) of similar M_n (~38 kg/mol) and D (~1.94).

The kinetic study of FRP of MA was also conducted based on the residence time by varying the flow rate in the same tubular reactor, as summarized in Figure 5 and Table S3. It can be seen from entries 1–3 that the M_n was initially increased up to \sim 76 kg/mol by raising the residence time by lowering the flow rate. However, after reaching a maximum limit of $M_n \approx 76$ kg/mol, it became irresponsive to the increase of residence time due to the characteristic kinetic behavior of a steady-state FRP in which chain terminations occur through disproportionation after acquiring a specific chain length.

We prepared a PMA homopolymer under similar reaction conditions in the batch using the same \sim 7 min reaction time (residence time for flow reactor) to compare the product with the material obtained from the continuous flow process (Figure S9; Table S4). It was observed that there is a good agreement in the characteristics (M_n and \mathcal{D}) between both products, which signifies that the experimental setup of this continuous flow reactor is suitable for the LRad reaction for these types of polar monomers.

Table 2. Radical polymerization of methyl acrylate in the presence of C1 catalyst in the continuous flow reactor

Entry ^a	Length of reactor (m)	Pump (1 and 2) flow rate (mL/min)	Res. Time (min)	Vol. of each solution (Cat. and MA) (mL)		Conc. of MA solution (mmol/mL)	Molmolar equiv of Cat.	M _n ^b (kg/mol)	Ðb	Yield (mg)	TOF (×1000/h)
1	5	0.15	13.3	4.5	2.1	5.58	2,655	76.09	1.93	494	2.73
2	5	0.30	6.6	9.0	2.1	5.58	2,655	47.57	1.92	535	2.96
3	10	0.30	13.3	9.0	2.1	5.58	2,655	72.02	1.94	994	2.75
4	10	0.30	13.3	9.0	1.4	5.58	3,983	118.86	1.96	914	3.79
5	10	0.30	13.3	9.0	2.1	2.79	1,328	37.82	1.96	490	1.36
6°	10	0.30	13.3	18.0	2.1	2.79	1,328	38.26	1.94	1,028	1.42

^aReaction conditions: 30 min reaction time, back pressure regulator = 40 psi.

^bMolecular weight (M_n) and dispersity (D) were determined by gel permeation chromatography (GPC) analysis with samples ran in THF at 40°C calibrated to polystyrene standards.

^c60 min reaction time.

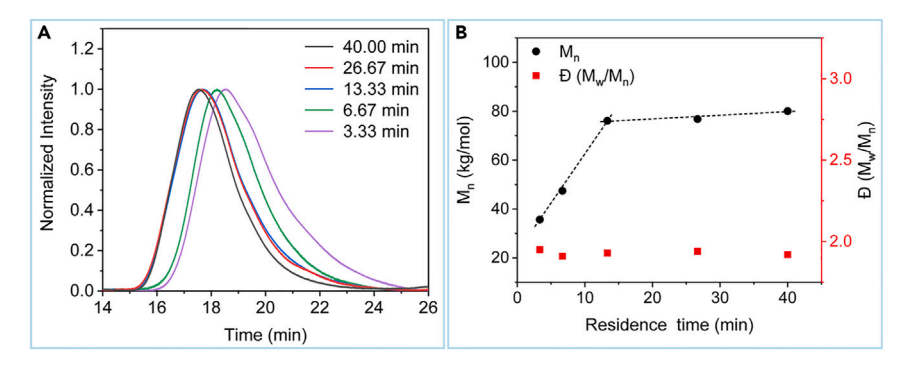


Figure 5. Kinetic study of PMA homopolymerization based on residence time varied with the flow rate of feed solutions (A) GPC traces of PMA homopolymers for different residence times (Table S3).

(B) M_n vs. residence time plot illustrates the increase in M_n of the polymer in relation to residence time.

Identity of macro-initiating radical species (radical trapping experiment)

After completing the study on PE and PMA homopolymerizations, we aimed to combine these two flow systems to synthesize PE-PA BCPs (PE-b-PMA), illustated in Figure 6. Herein, PE prepared through CIP is utilized as the precursor for further reaction progression to form the second block through FRP of acylate monomers (Figure S10). Therefore, we connected the continuous flow setups so that PE would form in the first reactor and then feed into the second reactor to react with MA, forming the Pd-PE-MA macrochelate. The presence of MeCN will facilitate the reopening of the macrochelate, which will consequently generate the PE-macroradical through Pd-C bond cleavage under blue light irradiation. This macroradical will then initiate the FRP in the presence of excess MA to form the BCPs. Initially, we worked with identical reaction conditions for the two reactors (entry 3 of Table 1 and entry 2 of Table 2), where both reactions were performed at the same flow rate (0.30 mL/min) with the same volume and concentration of catalyst solution (9.0 mL and 2.1 μ mol/mL), respectively.

However, to evidence the formation of macroradicals, which is the transition step from CIP to FRP, a TEMPO trapping experiment (Figure S11) was performed to capture the alkyl radical species formed in the light cycle (Figure S12). In contrast to comparable experiments in bulk, in which the macrochelate was isolated from the reaction mixture, and the TEMPO solution was added subsequently, TEMPO of the same amount (10 mol equiv with respect to the catalyst) was simply added to the MA solution. The ¹H-NMR analysis of the obtained product indicated that 84% of TEMPO-trapped products were formed with 16% chain transfer products (Figure S13; Table S5). These results aligned with comparable experiments conducted in bulk and confirmed the existence of PE macroradicals using TEMPO radical trapping as an analytics tool. ^{61,62} This experiment also gave a new perspective on possible simplifications of experimental setups in the bulk and opened the opportunity to perform MILRad functionalization reactions in the flow, in which functionalized TEMPO derivatives can be utilized for CRP of block segments.

Synthesis of PE-PA BCPs

A combination of characterization methods, such as size exclusion chromatography (SEC) or gel permeation chromatography (GPC), ¹H NMR spectroscopy, ¹H diffusion-ordered NMR spectroscopy (DOSY), small angle X-ray scattering (SAXS), and differential scanning calorimetry (DSC), were performed to analyze the PE-b-PMA BCP synthesized in the continuous flow (Figure 7; Table 3, entry 1). GPC traces of the crude PE-b-PMA (Figure 7A) indicated a mixture of the





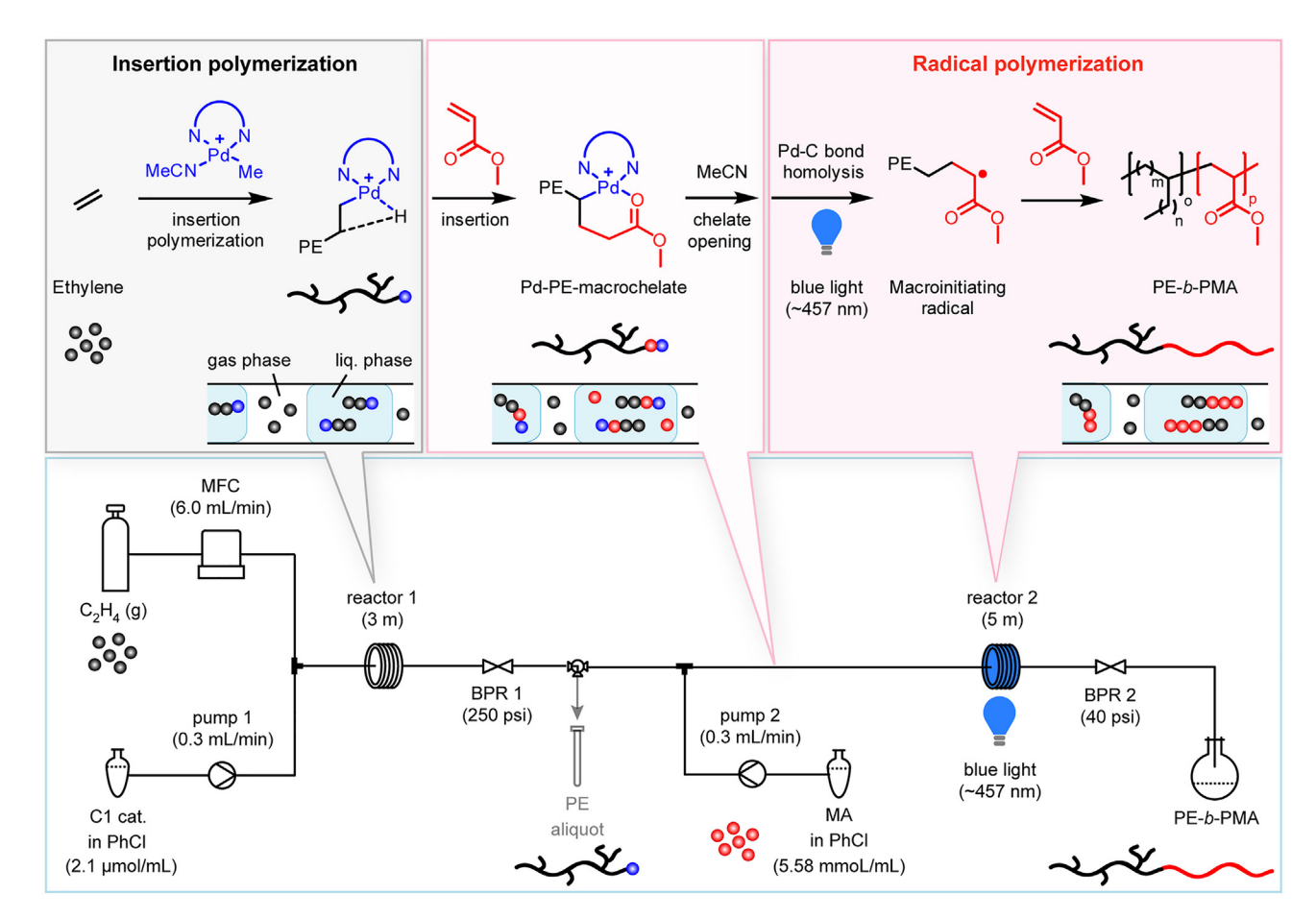


Figure 6. Schematic diagram of the synthesis of polyethylene-polyacrylate block copolymer in the continuous flow reactor

BCP and unreacted PE precursor. The M_n of the PE homopolymer was determined from the aliquot (14.60 kg/mol), which was utilized as a precursor for the BCP. The Mn of purified PE-b-PMA was 41.88 kg/mol with an overall 81% incorporation of MA determined from ¹H NMR spectroscopy (Figure S16). The ¹H DOSY NMR analysis of purified PE-b-PMA (Figure 7B) showed signals corresponding to PE block (1.25-0.83 ppm) and PMA block (3.66, 2.32, 1.97, and 1.68 ppm) aligned in a single diffusion coefficient. This observation confirmed that formed blocks were covalently bonded with each other. In addition, the SAXS profile of purified PE-b-PMA (Figures 7C and S27) portrayed principal scattering peaks evidencing the microphase separation (D = 56 nm, calculated as D spacing = $2 \pi n/q$) of two immiscible blocks arranged in a lamellar structure. Finally, the purified BCP was subjected to DSC analysis. Two separate glass transition temperatures (T_q) were observed in the obtained DSC traces (Figure 7D), which are in the range of the PE segment (-71°C) and PMA segment (9°C), indicating the presence of two heterogeneous phases in the same polymeric matrix. All of these findings collectively validate the successful combination of two different homopolymer segments prepared in a sequential continuous flow system.

One observation in the GPC trace of crude PE-b-PMA (Figure 7A) drew our attention to the fact that there was a significant extent of unconverted PE macrochelate in the obtained product. Our previous study suggested that the stable six-membered chelate formed by the acrylate monomer after the insertion must be opened by a

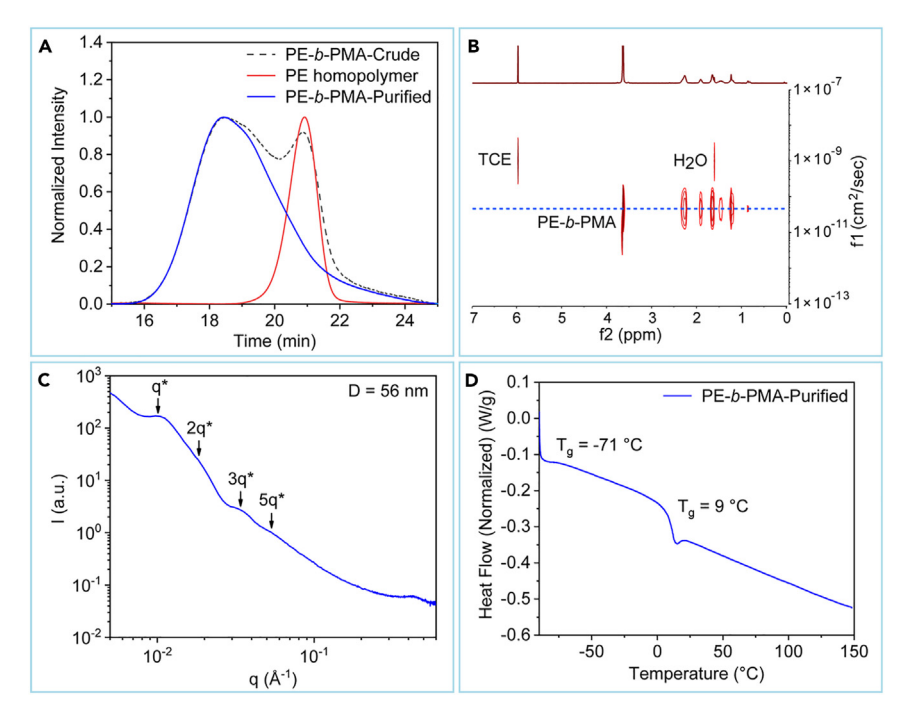


Figure 7. Characterization of synthesized PE-b-PMA in the continuous flow reactor

- (A) GPC traces of crude PE-b-PMA, PE homopolymer, and purified PE-b-PMA.
- (B) DOSY 1 H NMR spectrum in TCE ($C_{2}D_{2}CI_{4}$) at 25°C of purified PE-b-PMA.
- (C) SAXS data show principal scattering peaks of purified PE-b-PMA.
- (D) DSC of PE-b-PMA purified product.

Lewis base to enable an effective Pd-C bond homolysis under blue light irradiation.⁶¹ Therefore, the Lewis base (MeCN) plays a vital role in activting the polymer precursor to proceed to the BCP formation. However, an excess of MeCN also competes with monomers during the insertion and thus decreases the rate of polymerization. ^{67,71} To investigate this phenomenon, an additional amount of MeCN (5, 10, and 20 mol equiv to C1) was added to the MA solution during the formation of PE-b-PMA polymers of Table 3, entries 2, 3, and 4, respectively. The M_n of the macro-initiating PE were similar ~13.5 kg/mol for all the mentioned entries. Based on the analysis of the GPC traces of crude PE-b-PMA in Figures S15A-S15C, it is evident that the additional amount of MeCN facilitated the chelate opening efficiently so that the unreacted PE macroinitiator traces gradually became less prominent with better Đ due to more effective conversion from PE homopolymer to BCP. On the contrary, a gradual decrease in M_n and MA incorporation was also observed in the obtained GPC because of a reduction in the rate of polymerization. The increasing quantities of MeCN lead to an increased concentration of propagating chains that terminate more rapidly under the steady-state assumption in which the rate of initiation is equal to the rate of termination (Ri = Rt). For instance, without additional MeCN (entry 1), M_n was 41.88 kg/mol, whereas it decreased to 39.89, 38.57, and 23.19 kg/mol with an additional MeCN of 5, 10, and 20 mol equiv to C1. A similar trend was also observed for the MA incorporation of 70%, 61%, and 57% from 81%. To examine the BCPs prepared with additional ancillary ligands, we characterized the purified PE-b-PMA (Table 3, entry 2, additional MeCN = 5 mol equiv) by conducting ¹H DOSY, SAXS, and DSC analyses. ¹H DOSY NMR (Figure S23) of the purified PE-b-PMA sample recorded a single diffusion coefficient with corresponding PE and PMA signals. Additionally, the purified BCP depicted principal



Table 3. Polyethylene-polyacrylate block copolymers

			Excess ACN	PE homopolymer		Block copolymer		Acrylate			
Entry ^a	Acrylate	Sample	(mol equiv to cat.)	M _n ^b (kg/mol)	Ðb	M _n ^b (kg/mol)	Ðb	incorp. (mol %)	Yield (g)	<i>T</i> _g ^d (°C)	T _g ^d (°C)
1	MA	PE-b-PMA	0	14.60	1.07	41.88	1.93	81	345	-71	9
2	MA	PE-b-PMA	5	13.25	1.07	39.89	1.54	70	351	-69	9
3	MA	PE-b-PMA	10	13.52	1.07	38.57	1.52	61	342	-69	9
4	MA	PE-b-PMA	20	13.42	1.05	23.19	1.48	57	337	-66	9
5	EA	PE-b-PEA	5	12.09	1.05	52.06	1.92	66	360	-69	-17
6	n-BuA	PE-b-P(n-BuA)	5	12.32	1.05	144.69	1.67	82	957	N/A	-49
7	t-BuA	PE-b-P(t-BuA)	5	12.32	1.05	319.84	1.58	68	938	-66	31

 $^{^{}a}$ Reaction conditions: 0.3 mL/min pump flow rate (both pumps), 6.0 mL/min ethylene gas flow rate, 3 m tubular reactor with 250 psi back pressure regulator (at the end) for insertion polymerization, 5 m tubular reactor with 40 psi back pressure regulator (at the end) for radical polymerization, 2.10 μ mol/mL concentration of 2a catalyst, and 30 min reaction time.

scattering peaks corresponding to the microphase separation (D=36 nm) of two immiscible moieties with a lamellar microstructure in the SAXS experiment (Figure S28A). The analysis of the DSC traces (Figure S26A) showed two separate T_g 's in the range of the PE segment (-69° C) and PMA segment (9° C). Considering these outcomes, we can conclude that the addition of 5 mol equiv MeCN for this particular reaction condition is advantageous to result in a higher conversion of PE precursors forming BCPs through chain extension and incorporating acrylate blocks of the desired M_n .

To explore the versatility of our designed continuous flow system, different PE-b-PA BCPs were prepared through MILRad under the same reaction conditions as PE-b-PMA with additional MeCN (5 mol equiv), utilizing other acrylate monomers, such as ethyl acrylate (EA), n-butyl acrylate (n-BuA), and tert-butyl acrylate (t-BuA) (Table 3, entries 5, 6, and 7). Synthesized PE-b-PA BCPs were then purified and examined by similar characterization methods to confirm the desired BCP formation. The M_n of PE-b-PEA was found to be 52.06 kg/mol based on the GPC analysis (Table 3, entry 5) with an 66% EA incorporation determined from the corresponding ¹H NMR (Figure S20). ¹H DOSY NMR confirmed the formation of the di-block through covalent bonds by depicting the same diffusion coefficient for both PE and PEA signals (Figure S24). DSC traces of this BCP also showed separate T_a for PE and PEA segments at the characteristic temperatures -69°C and -17°C, respectively (Figure S26D). On the other hand, the purified PE-b-P(n-BuA) polymer showed a higher M_n (M_n = 144.69 kg/mol) with 82% acrylate incorporation (Table 3, entry 6). The corresponding peaks of PE and P(n-BuA) blocks accumulated around the same diffusion coefficient in ¹H DOSY NMR analysis (Figure S25), and the principal scattering peaks in SAXS trace (Figure S28B) with D spacing of 61 nm evident the formation of the desired BCP. Finally, the successful preparation of PE-b-P(t-BuA) was correspondingly confirmed by ¹H NMR and DSC experiments (Figures S22 and S26F), where the GPC analysis recorded a molecular weight of M_n = 319.84 kg/mol (Table 3, entry 7).

Conclusions

In summary, we developed a continuous flow reactor system that combines two adverse polymerization methods, CIP and FRP to form polar polyolefin BCPs in which a PA segment follows a PE segment. We demonstrated that the

^bMolecular weight (M_n) and dispersity (D) were determined by gel permeation chromatography (GPC) analysis with samples ran in THF at 40°C calibrated to polystyrene standards.

 $^{^{\}rm c} \rm Determined$ by $^{\rm 1} \rm H~NMR~in~CDCl_3$ at 25°C.

 $^{^{\}rm d}$ Glass transition temperature ($T_{\rm g}$) was determined by differential scanning calorimetry (DSC).





heterogeneous droplet flow is ideal because the gaseous phase is not only used to control the flow system dynamics but also carries the gaseous ethylene monomer. We could maintain a living CIP of ethylene in the continuous flow, and a systematic investigation of the influences of flow parameters on the corresponding M_n and yield of prepared PE homopolymers utilizing a diimine Pd^{II} complex was executed. This investigation additionally facilitated the preparation of PE homopolymers of any desired M_n without altering other flow conditions and experimental setups. The switch from one polymerization mechanism to the other was facilitated by the addition of acrylate monomers generating macrochelates and retarding the ethylene polymerization by irradiation of light and with the start of the radical pathway through the formation of macroradicals. Although ethylene is still present in the gaseous phase, it does not compete with the LRad pathway. TEMPO trapping experiments illustrated the successful formation of the PE macroinitiator by combining the two separate flow setups sequentially, which established the radical switch to form a PA segment. A broad range of M_n and compositions for PE-b-PMA was achieved on this platform, and several PE-PA BCPs were generated using different acrylate monomers. We demonstrated that the continuous flow polymer synthesis technique is a striking tool for producing these advanced polymeric materials through MILRad polymerization with precisely controlled architectures and desirable properties, which can pave the way for a wide range of applications.

EXPERIMENTAL PROCEDURES

Resource availability

Lead contact

Further information and requests for resources should be directed to and will be fulfilled by the lead contact, Eva Harth (harth@uh.edu).

Materials availability

All materials associated with the paper are either commercially available or can be prepared as indicated in the supplemental information, where full experimental details and characterization data are included.

Data and code availability

All data needed to support the conclusion of this manuscript are included in the main text or supplemental information.

Methods and setups of continuous flow reactors

Full experimental procedures and the setups of continuous flow reactors are provided in the supplemental information.

SUPPLEMENTAL INFORMATION

Supplemental information can be found online at https://doi.org/10.1016/j.chempr. 2024.05.016.

ACKNOWLEDGMENTS

The authors S.D.S. and E.H. thank the Robert A. Welch Foundation, USA for the generous support of this research (#H-E-0041 and #E-2066-202110327) through the Center of Excellence in Polymer Chemistry. The authors also gratefully acknowledge the National Science Foundation, USA for supporting parts of this work (CHEM-2108576). The authors thank Dr. Steve Swinnea for SAXS measurements at UT Austin.





AUTHOR CONTRIBUTIONS

S.D.S., H.D., and E.H. designed the study. E.H. supervised the study, and S.D.S. synthesized and characterized the compounds. S.D.S. and E.H. wrote the manuscript. All authors discussed the results and commented on the manuscript.

DECLARATION OF INTERESTS

The authors declare no competing interests.

Received: April 5, 2024 Revised: May 11, 2024 Accepted: May 21, 2024 Published: June 17, 2024

REFERENCES

- 1. Wiles, C., and Watts, P. (2008). Continuous Flow Reactors, a Tool for the Modern Synthetic Chemist. Eur. J. Org. Chem. 2008, 1655–1671. https://doi.org/10.1002/ejoc.200701041.
- Wilms, D., Klos, J., and Frey, H. (2008). Microstructured Reactors for Polymer Synthesis: A Renaissance of Continuous Flow Processes for Tailor-Made Macromolecules? Macromol. Chem. Phys. 209, 343–356. https://doi.org/10.1002/macp.200700588.
- Rossetti, I., and Compagnoni, M. (2016). Chemical reaction engineering, process design and scale-up issues at the frontier of synthesis: Flow chemistry. Chem. Eng. J. 296, 56–70. https://doi.org/10.1016/j.cej.2016. 02.119.
- Guidi, M., Seeberger, P.H., and Gilmore, K. (2020). How to approach flow chemistry. Chem. Soc. Rev. 49, 8910–8932. https://doi.org/10. 1039/C9C5008328
- Reis, M.H., Leibfarth, F.A., and Pitet, L.M. (2020). Polymerizations in Continuous Flow: Recent Advances in the Synthesis of Diverse Polymeric Materials. ACS Macro Lett. 9, 123–133. https://doi.org/10.1021/ acsmacrolett.9b00933.
- Zaquen, N., Rubens, M., Corrigan, N., Xu, J., Zetterlund, P.B., Boyer, C., and Junkers, T. (2020). Polymer Synthesis in Continuous Flow Reactors. Prog. Polym. Sci. 107, 101256. https://doi.org/10.1016/j.progpolymsci.2020. 101256.
- 7. Hone, C.A., and Kappe, C.O. (2021). Towards the Standardization of Flow Chemistry Protocols for Organic Reactions. Chemistry. Methods 1, 454–467. https://doi.org/10.1002/cmtd.202100059.
- Wegner, J., Ceylan, S., and Kirschning, A. (2011). Ten key issues in modern flow chemistry. Chem. Commun. (Camb) 47, 4583– 4592. https://doi.org/10.1039/COCC05060A.
- 9. Adamo, A., Beingessner, R.L., Behnam, M., Chen, J., Jamison, T.F., Jensen, K.F., Monbaliu, J.-C.M., Myerson, A.S., Revalor, E.M., Snead, D.R., et al. (2016). On-demand continuous-flow production of pharmaceuticals in a compact, reconfigurable system. Science 352, 61–67. https://doi.org/10.1126/science.aaf1337.

- Burange, A.S., Osman, S.M., and Luque, R. (2022). Understanding flow chemistry for the production of active pharmaceutical ingredients. iScience 25, 103892. https://doi. org/10.1016/j.isci.2022.103892.
- Porta, R., Benaglia, M., and Puglisi, A. (2016). Flow Chemistry: Recent Developments in the Synthesis of Pharmaceutical Products. Org. Process Res. Dev. 20, 2–25. https://doi.org/10. 1021/acs.oprd.5b00325.
- Reis, M.H., Varner, T.P., and Leibfarth, F.A. (2019). The Influence of Residence Time Distribution on Continuous-Flow Polymerization. Macromolecules 52, 3551–3557. https://doi.org/10.1021/acs.macromol.9b00454
- Morsbach, J., Müller, A.H.E., Berger-Nicoletti, E., and Frey, H. (2016). Living Polymer Chains with Predictable Molecular Weight and Dispersity via Carbanionic Polymerization in Continuous Flow: Mixing Rate as a Key Parameter. Macromolecules 49, 5043–5050. https://doi.org/10.1021/acs.macromol. 6b00975.
- Mastan, E., and He, J. (2017). Continuous Production of Multi-block Copolymers in a Loop Reactor: When Living Polymerization Meets Flow Chemistry. Macromolecules 50, 9173–9187. https://doi.org/10.1021/acs. macromol.7b01662.
- Corrigan, N., Zhernakov, L., Hashim, M.H., Xu, J., and Boyer, C. (2019). Flow mediated metalfree PET-RAFT polymerisation for upscaled and consistent polymer production. React. Chem. Eng. 4, 1216–1228. https://doi.org/10. 1039/C9RE00014C.
- Danckwerts, P.V. (1953). Continuous flow systems: Distribution of residence times. Chem. Eng. Sci. 2, 1–13. https://doi.org/10. 1016/0009-2509(53)80001-1.
- Metzner, A.B., and Reed, J.C. (1955). Flow of non-newtonian fluids—correlation of the laminar, transition, and turbulent-flow regions. AIChE J. 1, 434–440. https://doi.org/10.1002/ aic.690010409.
- Walsh, D.J., Schinski, D.A., Schneider, R.A., and Guironnet, D. (2020). General route to design polymer molecular weight distributions through flow chemistry. Nat. Commun. 11,

- 3094. https://doi.org/10.1038/s41467-020-16874-6.
- Paulus, R.M., Erdmenger, T., Becer, C.R., Hoogenboom, R., and Schubert, U.S. (2007). Scale-Up of Microwave-Assisted Polymerizations in Continuous-Flow Mode: Cationic Ring-Opening Polymerization of 2-Ethyl-2-oxazoline. Macromol. Rapid Commun. 28, 484–491. https://doi.org/10. 1002/marc.200600756.
- Russum, J.P., Jones, C.W., and Schork, F.J. (2004). Continuous Reversible Addition-Fragmentation Chain Transfer Polymerization in Miniemulsion Utilizing a Multi-Tube Reaction System. Macromol. Rapid Commun. 25, 1064– 1068. https://doi.org/10.1002/marc. 200400086.
- Wurm, F., Wilms, D., Klos, J., Löwe, H., and Frey, H. (2008). Carbanions on Tap – Living Anionic Polymerization in a Microstructured Reactor. Macromol. Chem. Phys. 209, 1106– 1114. https://doi.org/10.1002/macp. 200700613.
- lida, K., Chastek, T.Q., Beers, K.L., Cavicchi, K.A., Chun, J., and Fasolka, M.J. (2009). Living anionic polymerization using a microfluidic reactor. Lab Chip 9, 339–345. https://doi.org/ 10.1039/B810006C.
- Hornung, C.H., Guerrero-Sanchez, C., Brasholz, M., Saubern, S., Chiefari, J., Moad, G., Rizzardo, E., and Thang, S.H. (2011). Controlled RAFT Polymerization in a Continuous Flow Microreactor. Org. Process Res. Dev. 15, 593–601. https://doi.org/10.1021/ op1003314.
- Zhou, Y., Gu, Y., Jiang, K., and Chen, M. (2019). Droplet-Flow Photopolymerization Aided by Computer: Overcoming the Challenges of Viscosity and Facilitating the Generation of Copolymer Libraries. Macromolecules 52, 5611–5617. https://doi.org/10.1021/acs. macromol.9b00846.
- Corrigan, N., Manahan, R., Lew, Z.T., Yeow, J., Xu, J., and Boyer, C. (2018). Copolymers with Controlled Molecular Weight Distributions and Compositional Gradients through Flow Polymerization. Macromolecules 51, 4553– 4563. https://doi.org/10.1021/acs.macromol. 8b00673.

Chem Article



- Kim, J., and Lee, C.-S. (2018). Microfluidic Approaches for Designing Multifunctional Polymeric Microparticles from Simple Emulsions to Complex Particles. Microfluid.: Fundam. Devices Appl. 375–404. https://doi. org/10.1002/9783527800643.ch12.
- Lu, S., and Wang, K. (2019). Kinetic study of TBD catalyzed δ-valerolactone polymerization using a gas-driven droplet flow reactor. React. Chem. Eng. 4, 1189–1194. https://doi.org/10. 1039/C9RE00046A.
- Russum, J.P., Jones, C.W., and Schork, F.J. (2006). Impact of flow regime on polydispersity in tubular RAFT miniemulsion polymerization. AIChE J. 52, 1566–1576. https://doi.org/10. 1002/aic.10730.
- Zhou, Y., Fu, Y., and Chen, M. (2022). Facile Control of Molecular Weight Distribution via Droplet-Flow Light-Driven Reversible-Deactivation Radical Polymerization†. Chin. J. Chem. 40, 2305–2312. https://doi.org/10.1002/ cjoc.202200236.
- Zhou, Y., Han, S., Gu, Y., and Chen, M. (2021). Facile synthesis of gradient copolymers enabled by droplet-flow photo-controlled reversible deactivation radical polymerization. Sci. China Chem. 64, 844–851. https://doi.org/ 10.1007/s11426-020-9946-8.
- Ramsey, B.L., Pearson, R.M., Beck, L.R., and Miyake, G.M. (2017). Photo-induced Organocatalyzed Atom Transfer Radical Polymerization Using Continuous Flow. Macromolecules 50, 2668–2674. https://doi. org/10.1021/acs.macromol.6b02791.
- Wenn, B., Conradi, M., Carreiras, A.D., Haddleton, D.M., and Junkers, T. (2014). Photoinduced copper-mediated polymerization of methyl acrylate in continuous flow reactors. Polym. Chem. 5, 3053–3060. https://doi.org/ 10.1039/C3PY01762A.
- Chuang, Y.-M., Wenn, B., Gielen, S., Ethirajan, A., and Junkers, T. (2015). Ligand switch in photo-induced copper-mediated polymerization: synthesis of methacrylate– acrylate block copolymers. Polym. Chem. 6, 6488–6497. https://doi.org/10.1039/ C5PY00592B.
- Noda, T., Grice, A.J., Levere, M.E., and Haddleton, D.M. (2007). Continuous process for ATRP: Synthesis of homo and block copolymers. Eur. Polym. J. 43, 2321–2330. https://doi.org/10.1016/j.eurpolymj.2007. 03.010.
- Li, Z., Chen, W., Zhang, L., Cheng, Z., and Zhu, X. (2015). Fast RAFT aqueous polymerization in a continuous tubular reactor: consecutive synthesis of a double hydrophilic block copolymer. Polym. Chem. 6, 5030–5035. https://doi.org/10.1039/C5PY00847F.
- Rubens, M., Latsrisaeng, P., and Junkers, T. (2017). Visible light-induced iniferter polymerization of methacrylates enhanced by continuous flow. Polym. Chem. 8, 6496–6505. https://doi.org/10.1039/C7PY01157A.
- Zaquen, N., Kadir, A.M.N.B.P.H.A., Iasa, A., Corrigan, N., Junkers, T., Zetterlund, P.B., and Boyer, C. (2019). Rapid Oxygen Tolerant Aqueous RAFT Photopolymerization in Continuous Flow Reactors. Macromolecules

- 52, 1609–1619. https://doi.org/10.1021/acs.macromol.8b02628.
- Rosenfeld, C., Serra, C., O'Donohue, S., and Hadziioannou, G. (2007). Continuous Online Rapid Size Exclusion Chromatography Monitoring of Polymerizations - CORSEMP. Macro. Reaction Engineering 1, 547–552. https://doi.org/10.1002/mren.200700024.
- Rosenfeld, C., Serra, C., Brochon, C., and Hadziioannou, G. (2008). Influence of micromixer characteristics on polydispersity index of block copolymers synthesized in continuous flow microreactors. Lab Chip 8, 1682–1687. https://doi.org/10.1039/B803885F.
- Lauterbach, F., Rubens, M., Abetz, V., and Junkers, T. (2018). Ultrafast PhotoRAFT Block Copolymerization of Isoprene and Styrene Facilitated through Continuous-Flow Operation. Angew. Chem. Int. Ed. Engl. 57, 14260–14264. https://doi.org/10.1002/anie. 201809759.
- Nagaki, A., Tomida, Y., Miyazaki, A., and Yoshida, J.-i. (2009). Microflow System Controlled Anionic Polymerization of Alkyl Methacrylates. Macromolecules 42, 4384–4387. https://doi.org/10.1021/ma900551a.
- Nagaki, A., Miyazaki, A., and Yoshida, J.-i. (2010). Synthesis of Polystyrenes—Poly(alkyl methacrylates) Block Copolymers via Anionic Polymerization Using an Integrated Flow Microreactor System. Macromolecules 43, 8424–8429. https://doi.org/10.1021/ ma101663x.
- Nagaki, A., Takahashi, Y., Akahori, K., and Yoshida, J.-i. (2012). Living Anionic Polymerization of tert-Butyl Acrylate in a Flow Microreactor System and Its Applications to the Synthesis of Block Copolymers. Macro. Reaction Engineering 6, 467–472. https://doi. org/10.1002/mren.201200051.
- Kim, J.-S., Kweon, J.-O., Lee, J.-H., and Noh, S.-T. (2015). Synthesis of high molecular weight poly(styrene-b-methyl methacrylate) using a plug flow reactor system by anionic polymerization. Macromol. Res. 23, 100–110. https://doi.org/10.1007/s13233-015-3008-2.
- Nagaki, A., Takumi, M., Tani, Y., and Yoshida, J.-i. (2015). Polymerization of vinyl ethers initiated by dendritic cations using flow microreactors. Tetrahedron 71, 5973–5978. https://doi.org/10.1016/j.tet.2015.05.096.
- Zhu, N., Feng, W., Hu, X., Zhang, Z., Fang, Z., Zhang, K., Li, Z., and Guo, K. (2016). Organocatalyzed continuous flow ringopening polymerizations to homo- and blockpolylactones. Polymer 84, 391–397. https://doi. org/10.1016/j.polymer.2016.01.019.
- Zhu, N., Huang, W., Hu, X., Liu, Y., Fang, Z., and Guo, K. (2018). Enzymatic Continuous Flow Synthesis of Thiol-Terminated Poly(δ-Valerolactone) and Block Copolymers. Macromol. Rapid Commun. 39, e1700807. https://doi.org/10.1002/marc.201700807.
- Huang, W., Zhu, N., Liu, Y., Wang, J., Zhong, J., Sun, Q., Sun, T., Hu, X., Fang, Z., and Guo, K. (2019). A novel microfluidic enzymeorganocatalysis combination strategy for ringopening copolymerizations of lactone, lactide and cyclic carbonate. Chem. Eng. J. 356,

- 592–597. https://doi.org/10.1016/j.cej.2018. 09.033.
- Nagaki, A., Miyazaki, A., Tomida, Y., and Yoshida, J.-i. (2011). Anionic polymerization of alkyl methacrylates using flow microreactor systems. Chem. Eng. J. 167, 548–555. https:// doi.org/10.1016/j.cej.2010.07.073.
- Baeten, E., Haven, J.J., and Junkers, T. (2017). RAFT multi-block reactor telescoping: from monomers to tetrablock copolymers in a continuous multistage reactor cascade. Polym. Chem. 8, 3815–3824. https://doi.org/10.1039/ C7PY00585G.
- Vandenbergh, J., Tura, T., Baeten, E., and Junkers, T. (2014). Polymer end group modifications and polymer conjugations via "click" chemistry employing microreactor technology. J. Polym. Sci. Part A: Polym. Chem. 52, 1263–1274. https://doi.org/10.1002/pola. 27112.
- Zhu, N., Huang, W., Hu, X., Liu, Y., Fang, Z., and Guo, K. (2018). Chemoselective polymerization platform for flow synthesis of functional polymers and nanoparticles. Chem. Eng. J. 333, 43–48. https://doi.org/10.1016/j.cej.2017. 09 143
- Yoon, B.J., and Rhee, H.-K. (1985). A STUDY OF THE HIGH PRESSURE POLYETHYLENE TUBULAR REACTOR. Chem. Eng. Commun. 34, 253–265. https://doi.org/10.1080/ 00986448508911202.
- Machi, S., Kawakami, W., Yamaguchi, K., Hosaki, Y., Hagiwara, M., and Sugo, T. (1968). Structure and properties of polyethylene produced by γ-radiation polymerization in flow system. J. Appl. Polym. Sci. 12, 2639–2647. https://doi.org/10.1002/app.1968.070121206.
- Azmi, A., and Aziz, N. (2016). Simulation Studies of Low-density Polyethylene Production in a Tubular Reactor. Procedia Eng. 148, 1170– 1176. https://doi.org/10.1016/j.proeng.2016. 06.620
- Fernandes, F.A.N., and Ferrareso Lona, L.M. (2001). Fluidized-bed reactor modeling for polyethylene production. J. Appl. Polym. Sci. 81, 321–332. https://doi.org/10.1002/ app 1442
- Alves, R.F., Casalini, T., Storti, G., and McKenna, T.F.L. (2021). Gas-Phase Polyethylene Reactors—A Critical Review of Modeling Approaches. Macro. Reaction Engineering 15, 2000059. https://doi.org/10. 1002/mren.202000059.
- Chen, K., Zhou, Y., Han, S., Liu, Y., and Chen, M. (2022). Main-Chain Fluoropolymers with Alternating Sequence Control via Light-Driven Reversible-Deactivation Copolymerization in Batch and Flow. Angew. Chem. Int. Ed. Engl. 61, e202116135. https://doi.org/10.1002/anie. 202116135.
- Keyes, A., Basbug Alhan, H.E., Ha, U., Liu, Y.-S., Smith, S.K., Teets, T.S., Beezer, D.B., and Harth, E. (2018). Light as a Catalytic Switch for Block Copolymer Architectures: Metal–Organic Insertion/Light Initiated Radical (MILRad) Polymerization. Macromolecules 51, 7224– 7232. https://doi.org/10.1021/acs.macromol. 8b01719.
- 60. Keyes, A., Dau, H., Basbug Alhan, H.E., Ha, U., Ordonez, E., Jones, G.R., Liu, Y.-S., Tsogtgerel,





- E., Loftin, B., Wen, Z., et al. (2019). Metalorganic insertion light initiated radical (MILRad) polymerization: photo-initiated radical polymerization of vinyl polar monomers with various palladium diimine catalysts. Polym. Chem. 10, 3040-3047. https://doi.org/10.1039/
- 61. Dau, H., Keyes, A., Basbug Alhan, H.E., Ordonez, E., Tsogtgerel, E., Gies, A.P. Auyeung, E., Zhou, Z., Maity, A., Das, A., et al. (2020). Dual Polymerization Pathway for Polyolefin-Polar Block Copolymer Synthesis via MILRad: Mechanism and Scope. J. Am. Chem. Soc. 142, 21469-21483. https://doi.org/10. 1021/jacs.0c10588.
- 62. Keyes, A., Dau, H., Matyjaszewski, K., and Harth, E. (2022). Tandem Living Insertion and Controlled Radical Polymerization for Polyolefin-Polyvinyl Block Copolymers. Angew. Chem. Int. Ed. Engl. 61, e202112742. https://doi.org/10.1002/anie.202112742.
- 63. Guan, Z., Cotts, P.M., McCord, E.F., and McLain, S.J. (1999). Chain Walking: A New Strategy to Control Polymer Topology. Science 283, 2059-2062. https://doi.org/10.1126/ science.283.5410.2059.

- 64. Ittel, S.D., Johnson, L.K., and Brookhart, M. (2000). Late-Metal Catalysts for Ethylene Homo- and Copolymerization. Chem. Rev. 100, 1169-1204. https://doi.org/10.1021/ cr9804644.
- 65. Allen, K.E., Campos, J., Daugulis, O., and Brookhart, M. (2015). Living Polymerization of Ethylene and Copolymerization of Ethylene/ Methyl Acrylate Using "Sandwich" Diimine Palladium Catalysts. ACS Cat. 5, 456–464. https://doi.org/10.1021/cs5016029.
- 66. Gottfried, A.C., and Brookhart, M. (2001). Living Polymerization of Ethylene Using Pd(II) α-Diimine Catalysts. Macromolecules 34, 1140-1142. https://doi.org/10.1021/ ma001595l.
- 67. Gottfried, A.C., and Brookhart, M. (2003). Living and Block Copolymerization of Ethylene and α-Olefins Using Palladium(II)α-Diimine Catalysts. Macromolecules 36, 3085-3100. https://doi.org/10.1021/ ma025902u.
- 68. Johnson, L.K., Mecking, S., and Brookhart, M. (1996). Copolymerization of Ethylene and Propylene with Functionalized Vinyl Monomers

- by Palladium(II) Catalysts. J. Am. Chem. Soc. 118, 267-268. https://doi.org/10.1021/ ja953247i.
- 69. Mecking, S., Johnson, L.K., Wang, L., and Brookhart, M. (1998). Mechanistic Studies of the Palladium-Catalyzed Copolymerization of Ethylene and α -Olefins with Methyl Acrylate. J. Am. Chem. Soc. 120, 888–899. https://doi.org/10.1021/ja964144i.
- 70. Philipp, D.M., Muller, R.P., Goddard, W.A., Storer, J., McAdon, M., and Mullins, M. (2002). Computational Insights on the Challenges for Polymerizing Polar Monomers. J. Am. Chem. Soc. 124, 10198-10210. https://doi.org/10.1021/ ia0157705.
- 71. Jones, G.R., Basbug Alhan, H.E., Karas, L.J., Wu, J.I., and Harth, E. (2021). Switching the Reactivity of Palladium Diimines with "Ancillary" Ligand to Select between Olefin Polymerization, Branching Regulation, or Olefin Isomerization. Angew. Chem. Int. Ed. Engl. 60, 1635-1640. https://doi.org/10.1002/anie. 202012400.